POLITECNICO DI TORINO
Repository ISTITUZIONALE

Free-vibration analysis of laminated shells via refined MITC9 elements

(Article begins on next page)

20 April 2024

Free-vibration analysis of laminated shells via refined MITC9 elements

M. Cinefra[1]

(1) Department of Aeronautics and Space Engineering,
Politecnico di Torino, Turin, Italy

Author and address for Correspondence
Dr. Maria Cinefra
Research Assistant,
Department of Aeronautics and Space Engineering
Politecnico di Torino,
Corso Duca degli Abruzzi, 24,
10129 Torino, ITALY,
tel +39.011.546.6869, fax +39.011.564.6899
e.mail: maria.cinefra@polito.it

Abstract

This article presents the free-vibration analysis of composite shell structures with double-curvature geometry by means of a shell finite element with variable through-the-thickness kinematic. The refined models used are grouped in the Unified Formulation by Carrera (CUF) and they permit the distribution of displacements and stresses along the thickness of the multilayered shell to be accurately described. The shell element has nine nodes and the Mixed Interpolation of Tensorial Components (MITC) method is used to contrast the membrane and shear locking phenomenon. The governing equations are derived from the Principle of Virtual Displacements (PVD). Laminated cylindrical and spherical shells with simply-supported edges are analyzed. Various laminations, orthotropic ratios and thickness ratios are considered. The results, obtained with different theories contained in the CUF, are compared with both the elasticity solutions given in literature and the analytical solutions obtained using the CUF and the Navier's method. The shell element based on the CUF is very efficient and refined models provide better results than classical ones in the free-vibration analysis of multilayered composite shells. Finally, spherical shells with different boundary conditions are analyzed using various theories in order to provide FEM benchmark solutions.

1   Introduction

The subject of vibrations is fascinating and is continually acquiring greater importance in the modern science and engineering curriculum, as it plays an important role in almost every field of applied science today. At the same time, shell structures have a predominant role in a variety of engineering applications thanks to their efficient load-carrying capabilities and the continuous development of new structural materials, such as composite layered materials, leads to increasingly complex structural designs that require careful analysis.

The anisotropy as well as complicating effects, such as the C_z^0 - Requirements (zig-zag effects in the displacements and interlaminar continuity for the stresses) and the couplings between in-plane and out-of-plane strains, make the analysis of layered composite shells complicated in practice. Analytical, closed form solutions are available in very few cases. In most of the practical problems, the solution demand applications of approximated computational methods.

Selmane and Lakis [1],[2] have presented a method for the dynamic and static analysis of thin, elastic, anisotropic, and nonuniform open cylindrical shells. The open shells are assumed to be simply supported along their curved edges and to have arbitrary straight-edge boundary conditions. The method is a hybrid of finite element method and classical shell theories. Bardell et al. [3] have used the h-p version of the finite element method and made a detailed study of the vibration characteristics of completely free, open, and cylindrically curved isotropic shell panels. Singh [4] has presented the free vibration analysis of doubly-curved open deep sandwich shells made of thin outer layers of high strength and high density material and a relatively thick core of low strength low density material.The Rayleigh-Ritz method is used to obtain the natural frequencies. Lee and Han [5] have discussed the free vibration analysis of isotropic plates and shells using a nine-node degenerated shell element. In this analysis, first-order shear deformation theory has been used. Zhao et al. [6] have analyzed the vibration behavior of composite cylindrical panels by meshfree (meshless) approach. Also Tornabene et al. [7]-[10] have performed the free-vibration analysis of doubly-curved laminated composite and functionally-graded shells using meshless methods, such as the Generalized Differential Quadrature (GDQ) and the Radial Basis Functions (RBF) method. Hossain et al. [11] have presented an improved finite element model for the linear analysis of anisotropic and laminated doubly-curved moderately thick composite shell panels. The model has been developed by considering a first-order shear deformation theory. Liu et al. [12] have implemented the element free Galerkin method for static and free vibration analyses of

2

general shell structures. The formulation has been verified through numerical examples of spatial shell structures. Civalek [13]-[16] has used the discrete singular convolution (DSC) method and performed the free vibration analysis of laminated conical shells, rotating truncated conical shells and laminated composite conical and cylindrical shells. Malekzadeh et al. [17] have made the three-dimensional free vibration analysis of arbitrary laminated circular cylindrical shells using a mixed layer-wise theory and differential quadrature (DQ) method (LW-DQ).

Among the computational techniques implemented for the analysis of layered structures, a predominant role has been played by Finite Element Method (FEM). The most of finite elements available in literature are formulated on the bases of axiomatic-type theories, in which the unknown variables are postulated along the thickness. Various finite elements for composite shells were discussed by Carrera [18]. Thin shell elements were used to analyze the vibrations of composite shells by many researchers (Cyr et al. [19]; Lee and Saravanos [20]; Lakshminarayana and Dwarakanath [21]; Chen et al. [22]; Gotsis and Guptill [23]; Isaksson et al. [24]; Soares et al. [25]; Chang and Shyong [26]; Lakis and Sinno [27]). Thin and thick shallow shell elements were developed and used for composite shell vibration research in various studies (Beakou and Touratier [28]; Singh and Kumar [29]; Chakravorty et al. [30]-[32]; Argyris and Tenek [33]; Kapania and Mohan [34]; Kosmatka [35]; Zhu [36]). Vibration and damping analysis of pretwisted composite blades was performed by Nabi and Ganesan [37]. Predictor-corrector procedures for stress and free vibration analyses of multilayered composite plates and shells were performed by Noor et al. [38]. Sanders' shell theory was modified to include shear deformation and used to develop conforming finite elements by Abu-Farsakh and Qatu [39]. Hybrid-mixed formulations were used to study vibrations of composite shells (Wilt et al. [40]; Gendy et al. [41]). 3D elements were also used in the analysis of composite shells by Dasgupta and Huang [42]. Finally, nonlinear vibration analysis was performed by many researchers using various types of composite shell elements (Martin and Lung [43]; Lakis and Laveau [44]).

An improved doubly-curved shell finite element is here presented for the free-vibration analysis of composite structures. It is based on the Carrera's Unified Formulation (CUF), which was developed by Carrera for multi-layered structures [18],[45]. Both Equivalent Single Layer (ESL) and Layer Wise (LW) theories contained in the CUF are considered. The Mixed Interpolation of Tensorial Components (MITC) method [46]-[48] is used to contrast the membrane and shear locking because in [50] it was demonstrated that spurious zero energy modes are reduced in respect to other sub-integration techniques. The governing equations for the linear free-vibration analysis of composite structures are derived from the Principle of Virtual Displacements (PVD) in order to apply the finite element method. Cross-ply cylindrical and spherical shells with simply-supported edges are analyzed. The results, obtained with different models contained in the CUF, are compared with the exact solution given in literature and the analytical solution calculated with the Navier's method. Also FEM benchmark solutions regarding doubly-curved shells with different boundary conditions are provided.

2   Refined kinematic models

The refined models here considered are derived by means of the Unified Formulation by Carrera [51] (CUF). In the framework of the CUF, the displacement field is written by means of approximating functions in the thickness direction as follows:

$$\delta\boldsymbol{u}^k(\alpha,\beta,z) = F_\tau(z)\delta\boldsymbol{u}_\tau^k(\alpha,\beta); \qquad \boldsymbol{u}^k(\alpha,\beta,z) = F_s(z)\boldsymbol{u}_s^k(\alpha,\beta) \qquad \tau,s = 0,1,...,N \qquad (1)$$

where (α,β,z) is a curvilinear reference system, in which α and β are orthogonal and the curvature radii R_α and R_β are constant in each point of the domain Ω (see Figure 1). The displacement vector $\boldsymbol{u} = \{u,v,w\}$ has its components expressed in this system. $\delta\boldsymbol{u}$ indicates the virtual displacement

associated to the virtual work and k identifies the layer. F_τ and F_s are the so-called thickness functions depending only on z. $\boldsymbol{u}_s$ are the unknown variables depending on the coordinates α and β. τ and s are sum indexes and N is the order of expansion in the thickness direction assumed for the displacements.

In the case of Equivalent Single Layer (ESL) models, a Taylor expansion is employed as thickness functions:

$$\boldsymbol{u} = F_0\,\boldsymbol{u}_0 + F_1\,\boldsymbol{u}_1 + \ldots + F_N\,\boldsymbol{u}_N = F_s\,\boldsymbol{u}_s, \qquad s = 0, 1, \ldots, N. \tag{2}$$

$$F_0 = z^0 = 1, \quad F_1 = z^1 = z, \quad \ldots, \quad F_N = z^N. \tag{3}$$

Classical models, such as those based on the First-order Shear Deformation Theory (FSDT) [52], can be obtained from an ESL theory with $N = 1$, by imposing a constant transverse displacement through the thickness via penalty techniques. Also a model based on the hypotheses of Classical Lamination Theory (CLT) [53],[54] can be expressed by means of the CUF by applying a penalty technique to the constitutive equations (see section 4). This permits to impose that the transverse shear strains are null in the shell.

In the case of Layer-Wise (LW) models, the displacement is defined at k-layer level:

$$\boldsymbol{u}^k = F_t\,\boldsymbol{u}_t^k + F_b\,\boldsymbol{u}_b^k + F_r\,\boldsymbol{u}_r^k = F_s\,\boldsymbol{u}_s^k, \qquad s = t, b, r\,, \quad r = 2, ..., N. \tag{4}$$

$$F_t = \frac{P_0 + P_1}{2}, \quad F_b = \frac{P_0 - P_1}{2}, \quad F_r = P_r - P_{r-2}. \tag{5}$$

in which $P_j = P_j(\zeta_k)$ is the Legendre polynomial of j-order defined in the ζ_k-domain: $-1 \le \zeta_k \le 1$. The top (t) and bottom (b) values of the displacements are used as unknown variables and one can impose the following compatibility conditions:

$$u_t^k = u_b^{k+1}, \qquad k = 1, N_l - 1. \tag{6}$$

The LW models, in respect to the ESLs, allow the zig-zag form of the displacement distribution in layered structures to be modelled. It is possible to reproduce the zig-zag effects also in the framework of the ESL description by employing the Murakami theory. According to references [55], a zig-zag term can be introduced into equation (2) as follows:

$$\boldsymbol{u}^k = F_0\,\boldsymbol{u}_0 + \ldots + F_N\,\boldsymbol{u}_N + (-1)^k \zeta_k \boldsymbol{u}_Z. \tag{7}$$

Subscript Z refers to the introduced term. Such theories are called zig-zag (ZZ) theories.

3 MITC9 shell element

In this section, the derivation of a shell finite element for the analysis of multilayered structures is presented. The element is based on both the ESL, ZZ and LW theories contained in the Unified Formulation. A nine-nodes element with doubly-curved geometry is considered. After an overview in scientific literature about the methods that permit to withstand the membrane and shear locking, the MITC technique has been adopted for this element.

3.1 Doubly-curved shells

Shells are bi-dimensional structures in which one dimension (in general the thickness in z direction) is negligible with respect to the other two in-plane dimensions. Geometry and the reference system

are indicated in Figure 1. By considering multilayered structures, the square of an infinitesimal linear segment in the layer, the associated infinitesimal area and volume are given by:

$$ds_k^2 = \; H_\alpha^{k2} \, d\alpha_k^2 \; + \; H_\beta^{k2} \, d\beta_k^2 + H_z^{k2} \, dz_k^2 \,,$$

$$d\Omega_k = \; H_\alpha^k H_\beta^k \, d\alpha_k \, d\beta_k \,, \tag{8}$$

$$dV = \; H_\alpha^k \, H_\beta^k \, H_z^k \, d\alpha_k \, d\beta_k \, dz_k \,,$$

where the metric coefficients are:

$$H_\alpha^k = A^k(1 + z_k/R_\alpha^k), \quad H_\beta^k = B^k(1 + z_k/R_\beta^k), \quad H_z^k = 1 \,. \tag{9}$$

k denotes the k-layer of the multilayered shell; R_α^k and R_β^k are the principal radii of the midsurface of the layer k. A^k and B^k are the coefficients of the first fundamental form of Ω_k (Γ_k is the Ω_k boundary). In this paper, the attention has been restricted to shells with constant radii of curvature (cylindrical, spherical, toroidal geometries) for which $A^k = B^k = 1$. Details for shells are reported in [56].

Geometrical relations permit the in-plane ϵ_p^k and out-plane ϵ_n^k strains to be expressed in terms of the displacement $\boldsymbol{u}$. The following relations hold:

$$\epsilon_p^k = [\epsilon_{\alpha\alpha}^k, \epsilon_{\beta\beta}^k, \epsilon_{\alpha\beta}^k]^T = (\boldsymbol{D}_p^k + \boldsymbol{A}_p^k) \, \boldsymbol{u}^k \,, \quad \epsilon_n^k = [\epsilon_{\alpha z}^k, \epsilon_{\beta z}^k, \epsilon_{zz}^k]^T = (\boldsymbol{D}_{n\Omega}^k + \boldsymbol{D}_{nz}^k - \boldsymbol{A}_n^k) \, \boldsymbol{u}^k \,. \tag{10}$$

The explicit form of the introduced arrays is:

$$\boldsymbol{D}_p^k = \begin{bmatrix} \frac{\partial_\alpha}{H_\alpha^k} & 0 & 0 \\ 0 & \frac{\partial_\beta}{H_\beta^k} & 0 \\ \frac{\partial_\beta}{H_\beta^k} & \frac{\partial_\alpha}{H_\alpha^k} & 0 \end{bmatrix}, \quad \boldsymbol{D}_{n\Omega}^k = \begin{bmatrix} 0 & 0 & \frac{\partial_\alpha}{H_\alpha^k} \\ 0 & 0 & \frac{\partial_\beta}{H_\beta^k} \\ 0 & 0 & 0 \end{bmatrix}, \quad \boldsymbol{D}_{nz}^k = \begin{bmatrix} \partial_z & 0 & 0 \\ 0 & \partial_z & 0 \\ 0 & 0 & \partial_z \end{bmatrix}, \tag{11}$$

$$\boldsymbol{A}_p^k = \begin{bmatrix} 0 & 0 & \frac{1}{H_\alpha^k R_\alpha^k} \\ 0 & 0 & \frac{1}{H_\beta^k R_\beta^k} \\ 0 & 0 & 0 \end{bmatrix}, \quad \boldsymbol{A}_n^k = \begin{bmatrix} \frac{1}{H_\alpha^k R_\alpha^k} & 0 & 0 \\ 0 & \frac{1}{H_\beta^k R_\beta^k} & 0 \\ 0 & 0 & 0 \end{bmatrix}. \tag{12}$$

3.2 MITC method

Considering a 9-nodes finite element, the displacement components are interpolated on the nodes of the element by means of the Lagrangian shape functions N_i:

$$\delta\boldsymbol{u}_\tau = N_i\delta\boldsymbol{u}_{\tau_i} \qquad \boldsymbol{u}_s = N_j\boldsymbol{u}_{s_j} \qquad \text{with} \quad i,j = 1,...,9 \tag{13}$$

where $\boldsymbol{u}_{s_j}$ and $\delta\boldsymbol{u}_{\tau_i}$ are the nodal displacements and their virtual variations. Substituting in the geometrical relations (10) one has:

$$\begin{aligned} \epsilon_p &= F_\tau(\boldsymbol{D}_p + \boldsymbol{A}_p)(N_i\boldsymbol{I})\boldsymbol{u}_{\tau_i} \\ \epsilon_n &= F_\tau(\boldsymbol{D}_{n\Omega} - \boldsymbol{A}_n)(N_i\boldsymbol{I})\boldsymbol{u}_{\tau_i} + F_{\tau,z}(N_i\boldsymbol{I})\boldsymbol{u}_{\tau_i} \end{aligned} \tag{14}$$

where $\boldsymbol{I}$ is the identity matrix.

Considering the local coordinate system (ξ, η), the MITC shell elements ([57]-[59]) are formulated by using, instead of the strain components directly computed from the displacements, an interpolation of these within each element using a specific interpolation strategy for each component. The corresponding interpolation points, called *tying points*, are shown in Figure 2 for a nine-nodes element. Note that the transverse normal strain ϵ_{zz} is excluded from this procedure and it is directly calculated from the displacements.

The interpolating functions are Lagrangian functions and are arranged in the following arrays:

$$
\begin{aligned}
N_{m1} &= [N_{A1}, N_{B1}, N_{C1}, N_{D1}, N_{E1}, N_{F1}] \\
N_{m2} &= [N_{A2}, N_{B2}, N_{C2}, N_{D2}, N_{E2}, N_{F2}] \\
N_{m3} &= [N_P, N_Q, N_R, N_S]
\end{aligned}
\tag{15}
$$

From this point on, the subscripts $m1$, $m2$ and $m3$ indicate quantities calculated in the points $(A1, B1, C1, D1, E1, F1)$, $(A2, B2, C2, D2, E2, F2)$ and (P, Q, R, S), respectively. Therefore, the strain components are interpolated as follows:

$$
\begin{aligned}
\boldsymbol{\epsilon}_p &= \begin{bmatrix} \epsilon_{\alpha\alpha} \\ \epsilon_{\beta\beta} \\ \epsilon_{\alpha\beta} \end{bmatrix} = \begin{bmatrix} N_{m1} & 0 & 0 \\ 0 & N_{m2} & 0 \\ 0 & 0 & N_{m3} \end{bmatrix} \begin{bmatrix} \epsilon_{\alpha\alpha_{m1}} \\ \epsilon_{\beta\beta_{m2}} \\ \epsilon_{\alpha\beta_{m3}} \end{bmatrix} \\
\boldsymbol{\epsilon}_n &= \begin{bmatrix} \epsilon_{\alpha z} \\ \epsilon_{\beta z} \\ \epsilon_{zz} \end{bmatrix} = \begin{bmatrix} N_{m1} & 0 & 0 \\ 0 & N_{m2} & 0 \\ 0 & 0 & 1 \end{bmatrix} \begin{bmatrix} \epsilon_{\alpha z_{m1}} \\ \epsilon_{\beta z_{m2}} \\ \epsilon_{zz} \end{bmatrix}
\end{aligned}
\tag{16}
$$

where the strains $\epsilon_{\alpha\alpha_{m1}}$, $\epsilon_{\beta\beta_{m2}}$, $\epsilon_{\alpha\beta_{m3}}$, $\epsilon_{\alpha z_{m1}}$, $\epsilon_{\beta z_{m2}}$ are expressed by means of eq.s (14) in which the shape functions N_i and their derivatives are evaluated in the tying points. For example, one can considers the strain component $\epsilon_{\alpha\alpha}$ that is calculated as follows:

$$
\epsilon_{\alpha\alpha} = N_{A1}\epsilon_{\alpha\alpha_{A1}} + N_{B1}\epsilon_{\alpha\alpha_{B1}} + N_{C1}\epsilon_{\alpha\alpha_{C1}} + N_{D1}\epsilon_{\alpha\alpha_{D1}} + N_{E1}\epsilon_{\alpha\alpha_{E1}} + N_{F1}\epsilon_{\alpha\alpha_{F1}}
\tag{17}
$$

with:

$$
\epsilon_{\alpha\alpha_{A1}} = N_{i,\alpha}^{(A1)} F_\tau u_{\tau_i} + \frac{1}{H_\alpha R_\alpha} N_i^{(A1)} F_\tau w_{\tau_i}
\tag{18}
$$

The superscript $(A1)$ indicates that the shape function and its derivative are evaluated in the point of coordinates $(-\frac{1}{\sqrt{3}}, -\sqrt{\frac{3}{5}})$. Similar expressions can be written for $\epsilon_{\alpha\alpha_{B1}}, \epsilon_{\alpha\alpha_{C1}}, \epsilon_{\alpha\alpha_{D1}}, \epsilon_{\alpha\alpha_{E1}}, \epsilon_{\alpha\alpha_{F1}}$.

4 Constitutive equations

The second step towards the governing equations is the definition of the 3D constitutive equations that permit the stresses to be expressed by means of the strains. The generalized Hooke's law is considered, by employing a linear constitutive model for infinitesimal deformations. In a composite material, these

equations are obtained in material coordinates $(1, 2, 3)$ for each orthotropic layer k and then rotated in the general curvilinear reference system (α, β, z).

Therefore, the stress-strain relations after the rotation are:

$$
\begin{aligned}
\boldsymbol{\sigma}_p^k &= \{\sigma_{\alpha\alpha}^k, \sigma_{\beta\beta}^k, \sigma_{\alpha\beta}^k\} = \boldsymbol{C}_{pp}^k \, \boldsymbol{\epsilon}_p^k + \boldsymbol{C}_{pn}^k \, \boldsymbol{\epsilon}_n^k \\
\boldsymbol{\sigma}_n^k &= \{\sigma_{\alpha z}^k, \sigma_{\beta z}^k, \sigma_{zz}^k\} = \boldsymbol{C}_{np}^k \, \boldsymbol{\epsilon}_p^k + \boldsymbol{C}_{nn}^k \, \boldsymbol{\epsilon}_n^k
\end{aligned}
\tag{19}
$$

where

$$
\boldsymbol{C}_{pp}^k = \begin{bmatrix} C_{11}^k & C_{12}^k & C_{16}^k \\ C_{12}^k & C_{22}^k & C_{26}^k \\ C_{16}^k & C_{26}^k & C_{66}^k \end{bmatrix} \qquad \boldsymbol{C}_{pn}^k = \begin{bmatrix} 0 & 0 & C_{13}^k \\ 0 & 0 & C_{23}^k \\ 0 & 0 & C_{36}^k \end{bmatrix}
$$

$$
\boldsymbol{C}_{np}^k = \begin{bmatrix} 0 & 0 & 0 \\ 0 & 0 & 0 \\ C_{13}^k & C_{23}^k & C_{36}^k \end{bmatrix} \qquad \boldsymbol{C}_{nn}^k = \begin{bmatrix} C_{55}^k & C_{45}^k & 0 \\ C_{45}^k & C_{44}^k & 0 \\ 0 & 0 & C_{33}^k \end{bmatrix}
\tag{20}
$$

The material coefficients C_{ij} depend on the Young's moduli E_1, E_2, E_3, the shear moduli G_{12}, G_{13}, G_{23} and Poisson moduli ν_{12}, ν_{13}, ν_{23}, ν_{21}, ν_{31}, ν_{32} that characterize the material of the layer.

5 Free-vibration analysis

This section presents the derivation of the governing finite element stiffness matrix and mass matrix based on the PVD in the case of free-vibration analysis of multi-layered laminated shells.

The PVD for a multilayered doubly-curved shell is:

$$
\int_{\Omega_k} \int_{A_k} \left\{ \delta\boldsymbol{\epsilon}_p^{kT} \boldsymbol{\sigma}_p^k + \delta\boldsymbol{\epsilon}_n^{kT} \boldsymbol{\sigma}_n^k \right\} H_\alpha H_\beta \, d\Omega_k dz = \int_{\Omega_k} \int_{A_k} \rho^k \, \delta\boldsymbol{u} \, \ddot{\boldsymbol{u}} \, H_\alpha H_\beta \, d\Omega_k dz
\tag{21}
$$

where Ω_k and A_k are the integration domains on the midsurface and in the thickness direction, respectively. The member on the left hand side of the equation represents the variation of the internal work, while the member on the right hand side of the equation represents the kinetic energy due to the inertia. ρ stands for the density of the material, and $\ddot{\boldsymbol{u}}$ is the acceleration vector.

Substituting the constitutive equations (19), the geometrical relations written via the MITC method (16) and applying the Unified Formulation (1) and the FEM approximation (13), one obtains the following governing equations:

$$
\delta\boldsymbol{q}_{\tau_i}^k : \quad \boldsymbol{K}^{k\tau sij} \boldsymbol{q}_{s_j}^k = \boldsymbol{M}^{k\tau sij} \ddot{\boldsymbol{q}}_{s_j}^k
\tag{22}
$$

where $\boldsymbol{K}^{k\tau sij}$ is a 3×3 matrix, called fundamental nucleus, and its explicit expression is given in Appendix. This is the basic element from which the stiffness matrix of the whole structure is computed. The fundamental nucleus is expanded on the indexes τ and s in order to obtain the stiffness matrix of each layer. Then, the matrices of the layers are assembled at multi-layer level depending on the approach considered, ESL or LW. $\boldsymbol{M}^{k\tau sij}$ is the fundamental nucleus for the mass matrix and its components are:

$$
M_{\alpha\alpha}^{k\tau sij} = M_{\beta\beta}^{k\tau sij} = M_{zz}^{k\tau sij} = \rho^k \int_{\Omega_k} \int_{A_k} N_i N_j F_\tau F_s H_\alpha H_\beta \, dz \, d\Omega_k
$$

$$
M_{\alpha\beta}^{k\tau sij} = M_{\alpha z}^{k\tau sij} = M_{\beta z}^{k\tau sij} = M_{\beta\alpha}^{k\tau sij} = M_{z\alpha}^{k\tau sij} = M_{z\beta}^{k\tau sij} = 0
\tag{23}
$$

7

For more details about the derivation of governing equations, the reader can refer to the article [18]. The final form of the free-vibration problem can be written as it follows:

$$-\boldsymbol{M}\ddot{\boldsymbol{q}} + \boldsymbol{K}\boldsymbol{q} = 0 \tag{24}$$

where $\boldsymbol{q}$ is the vector of the nodal displacements. Introducing harmonic solutions, it is possible to compute the natural frequencies ω_l, by solving an eigenvalues problem:

$$-(\omega_l^2 \boldsymbol{M} + \boldsymbol{K})\boldsymbol{q}_l = 0 \tag{25}$$

where $\boldsymbol{q}_l$ is the l-th eigenvector.

6   Acronyms

Several refined and advanced two-dimensional models are contained in the Unified Formulation. Depending on the variables description (LW, ESL or ZZ) and the order of expansion N of the displacements in ξ_3, a large variety of kinematics shell theories can be obtained. A system of acronyms is given in order to denote these models. The first letter indicates the multi-layer approach which can be Equivalent Single Layer (E) or Layer Wise (L). The number N indicates the order of expansion used in the thickness direction (from 1 to 4). In the case of LW approach, the same order of expansion is used for each layer. In the case of ESL approach, a letter Z can be added if the zig-zag effects of displacements is considered by means of Murakami's zig-zag function. Summarizing, E1-E4 are ESL models. If Murakami zigzag function is used, these equivalent single layer models are indicated as EZ1-EZ3. In the case of layer wise approaches, the letter L is considered in place of E, so the acronyms are L1-L4. Classical theories such as Classical Lamination Theory (CLT) and First order Shear Deformation Theory (FSDT), can be obtained as particular cases of E1 theory simply imposing constant value of w through the thickness direction. An appropriate application of penalty technique to shear moduli of the material leads to CLT.

7   Numerical results

This section is composed of two parts. The first one is devoted to the assessment of the shell element based on the Unified Formulation by the free-vibration analysis of simply supported cylindrical and spherical shells. Using the theory that provides the most accurate results, the second part presents some benchmark solutions relative to spherical shells with particular boundary conditions.

7.1   Assessment

In order to assess the robustness of the present shell element and show the efficiency of CUF in the free-vibration analysis of laminated composites, some numerical results for simply-supported cross-ply cylindrical and spherical shells are presented. These are compared with the 3D solutions given in [60] for the cylindrical shell and the analytical solution ($\mathrm{L}4_a$) for the spherical panel. The analytical solution $\mathrm{L}4_a$ is obtained using the Principle of Virtual Displacements with a Layer-Wise approach of the fourth order and the Navier's method is employed to solve the governing equations in closed form. In [61], it was demonstrated that the $\mathrm{L}4_a$ solutions can be considered quasi-3D.

First, laminated circular cylinders are considered. The fibers of the top layer are running along the circumferential β direction while the fibers of the bottom layer are running along the longitudinal α direction. The material characteristics of the individual layers are those of typical high-modulus fibrous composites, namely $G_{LT}/E_T = 0.6$, $G_{TT}/E_T = 0.5$, $\nu_{LT} = \nu_{TT} = 0.25$, where the subscript L refer to

the direction of the fibers and the subscript T to the transverse direction. The results are given in terms of adimensional angular frequency. As a preliminary result, a convergence study has been performed in Table 1 considering different meshes for $E_L/E_T = 30$, $a/R_\beta = 1$, $h/R_\beta = 0.05$, $m = 1$ and $N_l = 2$, being a the axis length, N_l the number of layers and m is the number of axial half-waves. It can be noted that the 4×4 mesh is not sufficient to reach modes shapes with more than 2 circumferential half-waves, while the mesh 4×22 ensures the converge of the results for different orthotropic ratios and different half-waves; therefore, it has been adopted for the following analysis. The effect of degree of orthotropy of the individual layers of the cylindrical shell is studied, considering the following properties $a/R_\beta = 1$, $h/R_\beta = 0.2$, $N_l = 2$, $m = 1$ and $n = 4$, being n the number of circumferential half-waves. The results are compared with the 3D solutions by Noor and Rarig [60] (see Table 2). Different theories are considered and the results are in good agreement with the reference solutions. The effect of the thickness to radius ratio h/R has been also investigated in Table 3 for a cylindrical shell with $E_L/E_T = 30$, $a/R_\beta = 1$, $m = 1$ and $N_l = 2$. The results are given for various theories and for different circumferential half-wave numbers $n = 2, 4, 6$. The corresponding vibration modes are represented in Figures 3-5. It can be noted that, for thin shells $h/R = 0.05$, the exact solution is obtained with both higher order layer-wise and equivalent-single-layer theories, while for high thickness ratios, $h/R = 0.25$ and $h/R = 0.40$, only layer-wise theories can reach the reference solutions.

A final assessment is performed, studying the effect of the radius to the length ratio R/a, on a square multilayered spherical panel with the following properties: $E_L/E_T = 25$, $G_{LT}/E_T = 0.5$, $G_{TT}/E_T = 0.2$, $\nu_{LT} = \nu_{TT} = 0.25$, $a/h = 10$, $m = 1$, $n = 1$ and lamination $(0^o/90^o/0^o)$. A 16×16 mesh is employed in order to reach the exact solution. The results obtained with different theories are compared with some reference solutions: an analytical solution $L4_a$, an HSDT solution by Reddy and Liu [62], an FSDT solution by Reddy [63] and a CLT solution by Carrera [64]. The FEM results are in good agreement with the reference solutions, see Table 4.

7.2 FEM benchmark solutions

The spherical shells of the previous analysis are considered here with clamped/free/clamped/free boundary conditions. The effect of the radius to length ratio R/a and the radius to thickness ratio R/h has been investigated. The material properties and the lamination scheme are the same of the previous reference problems. A 16×16 mesh grid is employed. The results are given in terms of an adimensional natural frequency ω for the modal shape with $m = 1$ and $n = 1$, see Table 5.

8 Conclusions

This paper has dealt with the free-vibration analysis of composite cylindrical and spherical shells by means of a shell finite element based on the Unified Formulation by Carrera. An assessment of the element has been performed by analyzing cross-ply cylindrical and spherical shells with simply-supported boundary conditions. The results have been presented in terms of adimensional natural frequencies, for various thickness ratios, curvature ratios and orthotropic ratios. The performances of the shell element have been tested and the different theories (classical and refined) contained in the CUF have been compared. The conclusions that can be drawn are the following:

1. the shell element is locking-free when the shell is very thin and the results converge to the reference solution by increasing both the mesh and the order of expansion of the displacements in the thickness direction;

2. when the shell is very thick, the LW models work better than ZZ ones, and these work better than ESL models;

3. the classical models, such as CLT and FSDT fail in the free-vibration analysis of thick shells;

4. higher-order LW models provide very accurate results for both thick and thin multilayered shells, even though they increase the computational cost of the analysis.

Finally, some benchmark solutions have been provided for spherical shells that have not analytical reference solutions: lamination $(0^o, 90^o, 0^o)$ and clamped-free boundary conditions have been considered. Results have been presented in terms of adimensional natural frequencies. Future companion works will be devoted to the free-vibration analysis of anisotropic multilayered shells with various laminations and different types of loads will be considered.

References

[1] A. Selmane and A. A. Lakis, Influence of geometric nonlinearities on the free vibrations of orthotropic open cylindrical shells. *International Journal of Numerical Methods in Engineering*, 1997, 40(6), 1115-1137.

[2] A. Selmane and A. A. Lakis, Nonlinear dynamic analysis of orthotropic open cylindrical shells subjected to a flowing fluid. *Journal of Sound and Vibration*, 1997, 202(1), 67-93.

[3] N. S. Bardell, J. M. Dunsdon, and R. S. Langley, On the free vibration of completely free, open, cylindrically curved, isotropic shell panels, *Journal of Sound and Vibration*, 1997, 207(5), 647-669.

[4] A. V. Singh, Free vibration analysis of deep doubly curved sandwich panels, *Computers and Structures*, 1999, 73(1-5), 385-394.

[5] S. J. Lee and S. E. Han, Free-vibration analysis of plates and shells with a nine-node assumed natural degenerated shell element, *Journal of Sound and Vibration*, 2001, 241(4), 605-633.

[6] X. Zhao, K. M. Liew, and T. Y. Ng, Vibration analysis of laminated composite cylindrical panels via a meshfree approach, *International Journal of Solids and Structures*, 2003, 40(1), 161-180.

[7] F. Tornabene, E. Viola and N. Fantuzzi, General higher-order equivalent single layer theory for free vibrations of doubly-curved laminated composite shells and panels, *Composite Structures*, 2013, 104(1), 94-117.

[8] F. Tornabene, N. Fantuzzi, E. Viola and A. J. M. Ferreira, Radial basis function method applied to doubly-curved laminated composite shells and panels with a General Higher-order Equivalent Single Layer formulation, *Composites Part B: Engineering*, 2013, 55(1), 642659.

[9] F. Tornabene, N. Fantuzzi and M. Bacciocchi, The local GDQ method applied to general higher-order theories of doubly-curved laminated composite shells and panels: The free vibration analysis, *Composite Structures*, 2014, 116(1), 637-660.

[10] F. Tornabene, N. Fantuzzi and M. Bacciocchi, Free vibrations of free-form doubly-curved shells made of functionally graded materials using higher-order equivalent single layer theories, *Composites Part B: Engineering*, 2014, 67(1), 490-509.

[11] S. J. Hossain, P. K. Sinha, and A. H. Sheikh, A finite element formulation for the analysis of laminated composite shells, *Computers and Structures*, 2004, 82(20-21), 16231638.

[12] L. Liu, L. P. Chua, and D. N. Ghista, Element-free Galerkin method for static and dynamic analysis of spatial shell structures, *Journal of Sound and Vibration*, 2006, 95(1-2), 388406.

[13] O. Civalek, The determination of frequencies of laminated conical shells via the discrete singular convolution method, *Journal of Mechanics of Materials and Structures*, 2006, 1(1), 163181.

[14] O. Civalek, An efficient method for free vibration analysis of rotating truncated conical shells, Pressure Vessels and Piping, Vol. 83(1), 2006, pp. 1-12.

[15] O. Civalek, Numerical analysis of free vibrations of laminated composite conical and cylindrical shells: Discrete singular convolution (DSC) approach, *Journal of Computational and Applied Mathematics*, 2007, 205(1), 251-271.

[16] O. Civalek, Vibration analysis of laminated composite conical shells by the method of discrete singular convolution based on the shear deformation theory, *Composite B*, 2013, 45, 10011009.

[17] P. Malekzadeh, M. Farid, and P. Zahedinejad, A three-dimensional layerwise-differential quadrature free vibration analysis of laminated cylindrical shells, *International Journal of Pressure Vessels and Piping*, 2008, 85(7), 450458.

[18] E. Carrera, Theories and finite elements for multilayered anisotropic composite plates and shells, *Archives of Computational Methods in Engineering*, 2002, 9, 87-140.

[19] G. J. Cyr, R. L. Hinrichsen and R. A. Walley, Effects of cutouts on the dynamic response of curved rectangular composite panels, *AIAA Journal*, 1988, 26(5), 582-588.

[20] H. J. Lee and D. A. Saravanos, Mixed multi-field FE formulation for thermopiezoelectric composite shells, *International Journal of Solids and Structures*, 2000, 37(36), 4949-4967.

[21] H. V. Lakshminarayana and K. Dwarakanath, Free vibration characteristics of cylindrical shells made of composite material, *Journal of Sound and Vibrations*, 1992, 154(3), 431439.

[22] C. I. Chen, V. H. Mucino and E. J. Barbero, Finite element vibration analysis of a helically wound tubular and laminated composite material beam, *Computers and Structures*, 1993, 49(3), 399410.

[23] P. K. Gotsis and J. D. Guptill, Free vibration of fiber composite thin shells in a hot environment, *Journal of Reinforced Plastics and Composites*, 1995, 14(2), 143163.

[24] A. Isaksson, H. O. Saldner and N. E. Molin, Influence of enclosed air on vibration modes of a shell structure, Journal of Sound and Vibration, 1995, 187(3), 451466.

[25] C. M. M. Soares, V. F. Correia, H. Mateus and J. Herskovits, Discrete model for the optimal design of thin composite plate-shell type structures using a two-level approach, *Composite Structures*, 1995, 30(2), 147-157.

[26] J. S. Chang and J. W. Shyong, Thermally induced vibration of laminated circular cylindrical shell panels, Composite Sciencies and Technology, 1994, 51(3), 419427.

[27] A. A. Lakis and M. Sinno, Free vibration of axisymmetric and beam-like cylindrical shells, partially filled with liquid, *International Journal for Numerical Methods in Engineering*, 1992, 33(2), 235268.

[28] A. Beakou and M. Touratier, Rectangular FE for analysing composite multilayered shallow shells in statics, vibration and buckling, *International Journal for Numerical Methods in Engineering* 1993, 36(4), 627-653.

[29] A. V. Singh and V. Kumar, Vibration of laminated shallow shells on quadrangular boundary, *Journal of Aerospace Engineering*, 1996, 9(2), 52-57.

[30] D. Chakravorty, J. N. Bandyopadhyay and P. K. Sinha, Finite element free vibration analysis of point supported laminated composite cylindrical shells, *Journal of Sound and Vibration*, 1995, 181(1), 43-52.

[31] D. Chakravorty, J. N. Bandyopadhyay and P. K. Sinha, Free vibration analysis of point-supported laminated composite doubly curved shells: a FE approach, *Computers and Structures*, 1995, 54(2), 191-198.

[32] D. Chakravorty, J. N. Bandyopadhyay and P. K. Sinha, Finite element free vibration analysis of doubly-curved laminated composite shells, *Journal of Sound and Vibration*, 1996, 191(4), 491-504.

[33] J. Argyris and L. Tenek, Natural mode method: a practicable and novel approach to the global analysis of laminated composite plates and shells, *Applied Mechanics Reviews*, 1996, 49(7), 381-399.

[34] P. K. Kapania and P. Mohan, Static, free vibration and thermal analysis of composite plates and shells using a flat triangular shell element, *Computational Mechanics*, 1996, 17(5), 343-357.

[35] J. B. Kosmatka, Accurate shear-deformable six-node triangular plate element for laminated composite structures, *International Journal for Numerical Methods in Engineering*, 1994, 37(3), 431-455.

[36] J. Zhu, Free vibration analysis of multilayered composite plates and shells with the natural approach, *Computer Methods in Applied Mechanics and Engineering*, 1996, 130(1/2), 133-149.

[37] S. M. Nabi and N. Ganesan, Vibration and damping analysis of pre-twisted composite blades, *Computers and Structures*, 1993, 47(2), 275280.

[38] A.K. Noor, W. S. Burton and J. M. Peters, Predictor-corrector procedures for stress and free vibration analyses of multilayered composite plates and shells, *Computer Methods in Applied Mechanics and Engineering*, 1990, 82(1-3), 341-363.

[39] G. Abu-Farsakh and M. S. Qatu, A triangular conforming element for laminated shells, *Thin-Walled Structures*, 1995, 21(1), 31-42.

[40] T. E. Wilt, A. F. Saleeb and T. Y. Chang, Mixed element for laminated plates and shells, *Computers and Structures*, 1990, 37(4), 597-611.

[41] A. S. Gendy, A. F. Saleeb and S. N. Mikhail, Free vibrations and stability analysis of laminated composite plates and shells with hybrid-mixed formulation, *Computers and Structures*, Vol. 1997, 63(6), 1149-1163.

[42] A. Dasgupta and K. H. Huang, Layer-wise analysis for free vibrations of thick composite spherical panels, *Journal of Composite Materials*, 1997, 31(7), 658-671.

[43] C. W. Martin and S. F. Lung, Finite dynamic element for laminated composite plates and shells, *Computers and Structures*, 1991, 40(5), 12491259.

[44] A. A. Lakis and A. Laveau, Non-linear dynamic analysis of anisotropic cylindrical shells containing a flowing fluid, *International Journal of Solids and Structures*, 1991, 28(9), 10791094.

[45] E. Carrera, Theories and finite elements for multilayered plates and shells: a unified compact formulation with numerical assessment and benchmarking, *Archives of Computational Methods in Engineering*, 2003, 10(3), 215-296.

[46] K.-J. Bathe and E. N. Dvorkin, A four node plate bending element based on Mindlin/Reissner plate theory and mixed interpolation, *International Journal for Numerical Methods in Engineering*, 1985, 21, 367-383.

[47] K.-J. Bathe, F. Brezzi and S. W. Cho, The MITC7 and MITC9 plate elements, *Computers and Structures*, 1989, 32, 797-814.

[48] K.-J. Bathe, P. S. Lee and J. F. Hiller, Towards improving the MITC9 shell element, *Computers and Structures*, 2003, 81, 477-489.

[49] C. Chinosi and L. Della Croce, Mixed-interpolated elements for thin shell, *Communications in Numerical Methods in Engineering*, 1998, 14, 1155-1170.

[50] E. Carrera, M. Cinefra and P. Nali, MITC technique extended to variable kinematic multilayered plate elements, *Composite Structures*, 2010, 92(8), 18881895.

[51] E. Carrera, A class of two-dimensional theories for anisotropic multilayered plates analysis, *Accademia delle Scienze di Torino, Memorie Scienze Fisiche*, 1995, 19-20, 1-39.

[52] P. M. Naghdi, The theory of shells and plates, *Handbuch der Physic*, 1972, 4, 425-640.

[53] W. T. Koiter, On the foundations of the linear theory of thin elastic shell, *Proc. Kon. Nederl. Akad. Wetensch.*, 1970, 73, 169-195.

[54] P. G. Ciarlet and L. Gratie, Another approach to linear shell theory and a new proof of Korn's inequality on a surface, *C. R. Acad. Sci. Paris, Ser. I*, 2005, 340, 471-478.

[55] H. Murakami, Laminated composite plate theory with improved in-plane responses, *Journal of Applied Mechanics*, 1986, 53, 661-666.

[56] N.N. Rogacheva, The theory of piezoelectric Shells and Plates, CRC Press, Boca Raton, Florida (USA), 1994.

[57] D. Chapelle and K.-J.Bathe, The finite element analysis of shells.-Fundamentals, Springer, Berlin, 2003.

[58] K.-J. Bathe and E. Dvorkin, A formulation of general shell elements - the use of mixed interpolation of tensorial components, *International Journal for Numerical Methods in Engineering*, 1986, 22, 697-722.

[59] M. L. Bucalem and K.-J. Bathe, Higher-order MITC general shell elements, *International Journal for Numerical Methods in Engineering*, 1993, 36, 3729-3754.

[60] A. K. Noor and P. L. Rarig, Three-Dimensional solutions of laminated cylinders, *Computer Methods in Applied Mechanics and Engineering*, 1974, 3, 319-334.

[61] G. Giunta, F. Biscani, S. Belouettar and E. Carrera, Hierarchical modelling of doubly curved laminated composite shells under distributed and localised loadings, *Composites Part B: Engineering*, 2011, 42(4), 682-691.

[62] J.N. Reddy and C.F. Liu, A Higher-Order Shear Deformation Theory of Laminated Elastic Shells, *International Journal of Engineering Sciences*, 1985, 23, 319-330.

[63] J. N. Reddy, Exact Solution of Moderately Thick Laminated Shells, *Journal of Engineering Mechanics, ASCE*, 1984, 110, 769-809.

[64] E. Carrera, The Effects of Shear Deformation and Curvature on Buckling and Vibrations of Cross-ply Laminated Composite Shells, *Journal of Sound and Vibration*, 1991, 150(3), 405-433.

Appendix

In order to write the fundamental nucleus $\boldsymbol{K}^{k\tau sij}$ in compact form, the following integrals in the domain Ω_k are defined:

$$\left(W^k_{m1\,n1} \,;\, W^k_{m1\,n2} \,;\, W^k_{m2\,n1} \,;\, W^k_{m2\,n2} \right) = \int\limits_{\Omega_k} \left(N_{m1}N_{n1} \,;\, N_{m1}N_{n2} \,;\, N_{m2}N_{n1} \,;\, N_{m2}N_{n2} \right) d\alpha_k d\beta_k \qquad (26)$$

$$\left(W_{m1\,n3}^{k}\,;\,W_{m3\,n1}^{k}\,;\,W_{m3\,n3}^{k}\,;\,W_{m2\,n3}^{k}\,;\,W_{m3\,n2}^{k}\right)=\int\limits_{\Omega_{k}}\left(N_{m1}N_{n3}\,;\,N_{m3}N_{n1}\,;\,N_{m3}N_{n3}\,;\,N_{m2}N_{n3}\,;\,N_{m3}N_{n2}\right)d\alpha_{k}d\beta_{k}$$

$$(27)$$

$$\left(W_{m1\,j}^{k}\,;\,W_{m2\,j}^{k}\,;\,W_{m3\,j}^{k}\right)=\int\limits_{\Omega_{k}}\left(N_{m1}N_{j}\,;\,N_{m2}N_{j}\,;\,N_{m3}N_{j}\right)d\alpha_{k}d\beta_{k} \qquad (28)$$

$$\left(W_{i\,n1}^{k}\,;\,W_{i\,n2}^{k}\,;\,W_{i\,n3}^{k}\,;\,W_{ij}^{k}\right)=\int\limits_{\Omega_{k}}\left(N_{i}N_{n1}\,;\,N_{i}N_{n2}\,;\,N_{i}N_{n3}\,;\,N_{i}N_{j}\right)d\alpha_{k}d\beta_{k} \qquad (29)$$

$$\left(W_{m1\,j,\alpha}^{k}\,;\,W_{m1\,j,\beta}^{k}\,;\,W_{m2\,j,\alpha}^{k}\,;\,W_{m2\,j,\beta}^{k}\right)=\int\limits_{\Omega_{k}}\left(N_{m1}\frac{\partial N_{j}}{\partial\alpha}\,;\,N_{m1}\frac{\partial N_{j}}{\partial\beta}\,;\,N_{m2}\frac{\partial N_{j}}{\partial\alpha}\,;\,N_{m2}\frac{\partial N_{j}}{\partial\beta}\right)d\alpha_{k}d\beta_{k} \quad (30)$$

$$\left(W_{i,\alpha\,n1}^{k}\,;\,W_{i,\beta\,n1}^{k}\,;\,W_{i,\alpha\,n2}^{k}\,;\,W_{i,\beta\,n2}^{k}\right)=\int\limits_{\Omega_{k}}\left(\frac{\partial N_{i}}{\partial\alpha}N_{n1}\,;\,\frac{\partial N_{i}}{\partial\beta}N_{n1}\,;\,\frac{\partial N_{i}}{\partial\alpha}N_{n2}\,;\,\frac{\partial N_{i}}{\partial\beta}N_{n2}\right)d\alpha_{k}d\beta_{k} \qquad (31)$$

Moreover, the integrals on the domain A_{k}, in the thickness direction, are written as:

$$\left(J^{k\tau s},J_{\alpha}^{k\tau s},J_{\beta}^{k\tau s},J_{\frac{\alpha}{\beta}}^{k\tau s},J_{\frac{\beta}{\alpha}}^{k\tau s},J_{\alpha\beta}^{k\tau s}\right)=\int\limits_{A_{k}}F_{\tau}F_{s}\left(1,H_{\alpha}^{k},H_{\beta}^{k},\frac{H_{\alpha}^{k}}{H_{\beta}^{k}},\frac{H_{\beta}^{k}}{H_{\alpha}^{k}},H_{\alpha}^{k}H_{\beta}^{k}\right)dz \qquad (32)$$

$$\left(J^{k\tau_{z}s},J_{\alpha}^{k\tau_{z}s},J_{\beta}^{k\tau_{z}s},J_{\frac{\alpha}{\beta}}^{k\tau_{z}s},J_{\frac{\beta}{\alpha}}^{k\tau_{z}s},J_{\alpha\beta}^{k\tau_{z}s}\right)=\int\limits_{A_{k}}\frac{\partial F_{\tau}}{\partial z}F_{s}\left(1,H_{\alpha}^{k},H_{\beta}^{k},\frac{H_{\alpha}^{k}}{H_{\beta}^{k}},\frac{H_{\beta}^{k}}{H_{\alpha}^{k}},H_{\alpha}^{k}H_{\beta}^{k}\right)dz \qquad (33)$$

$$\left(J^{k\tau s_{z}},J_{\alpha}^{k\tau s_{z}},J_{\beta}^{k\tau s_{z}},J_{\frac{\alpha}{\beta}}^{k\tau s_{z}},J_{\frac{\beta}{\alpha}}^{k\tau s_{z}},J_{\alpha\beta}^{k\tau s_{z}}\right)=\int\limits_{A_{k}}F_{\tau}\frac{\partial F_{s}}{\partial z}\left(1,H_{\alpha}^{k},H_{\beta}^{k},\frac{H_{\alpha}^{k}}{H_{\beta}^{k}},\frac{H_{\beta}^{k}}{H_{\alpha}^{k}},H_{\alpha}^{k}H_{\beta}^{k}\right)dz \qquad (34)$$

$$\left(J^{k\tau_z s_z}, J^{k\tau_z s_z}_\alpha, J^{k\tau_z s_z}_\beta, J^{k\tau_z s_z}_{\frac{\alpha}{\beta}}, J^{k\tau_z s_z}_{\frac{\beta}{\alpha}}, J^{k\tau_z s_z}_{\alpha\beta} \right) = \int\limits_{A_k} \frac{\partial F_\tau}{\partial z} \frac{\partial F_s}{\partial z} \left(1, H^k_\alpha, H^k_\beta, \frac{H^k_\alpha}{H^k_\beta}, \frac{H^k_\beta}{H^k_\alpha}, H^k_\alpha H^k_\beta \right) dz \quad (35)$$

The fundamental nucleus $\boldsymbol{K}^{k\tau sij}$ is a (3×3) matrix and the explicit expression of its components is:

$$K^{k\tau sij}_{\alpha\alpha} = C^k_{55} N^{(m1)}_i N^{(n1)}_j W^k_{m1\,n1} J^{k\tau_z s_z}_{\alpha\beta} - \frac{C^k_{55}}{R^k_\alpha} N^{(m1)}_i N^{(n1)}_j W^k_{m1\,n1} J^{k\tau_z s}_\beta - \frac{C^k_{55}}{R^k_\alpha} N^{(m1)}_i N^{(n1)}_j W^k_{m1\,n1} J^{k\tau s_z}_\beta +$$
$$+ C^k_{66} N^{(m3)}_{i,\beta} N^{(n3)}_{j,\beta} W^k_{m3\,n3} J^{k\tau s}_{\frac{\alpha}{\beta}} + C^k_{16} N^{(m1)}_{i,\alpha} N^{(n3)}_{j,\beta} W^k_{m1\,n3} J^{k\tau s} + C^k_{16} N^{(m3)}_{i,\beta} N^{(n1)}_{j,\alpha} W^k_{m3\,n1} J^{k\tau s} +$$
$$+ C^k_{11} N^{(m1)}_{i,\alpha} N^{(n1)}_{j,\alpha} W^k_{m1\,n1} J^{k\tau s}_{\frac{\beta}{\alpha}} + \frac{C^k_{55}}{\left(R^k_\alpha\right)^2} N^{(m1)}_i N^{(n1)}_j W^k_{m1\,n1} J^{k\tau s}_{\frac{\beta}{\alpha}}$$
$$(36)$$

$$K^{k\tau sij}_{\alpha\beta} = C^k_{45} N^{(m1)}_i N^{(n2)}_j W^k_{m1\,n2} J^{k\tau_z s_z}_{\alpha\beta} - \frac{C^k_{45}}{R^k_\beta} N^{(m1)}_i N^{(n2)}_j W^k_{m1\,n2} J^{k\tau_z s}_\alpha - \frac{C^k_{45}}{R^k_\alpha} N^{(m1)}_i N^{(n2)}_j W^k_{m1\,n2} J^{k\tau s_z}_\beta +$$
$$+ C^k_{26} N^{(m3)}_{i,\beta} N^{(n2)}_{j,\beta} W^k_{m3\,n2} J^{k\tau s}_{\frac{\alpha}{\beta}} + C^k_{12} N^{(m1)}_{i,\alpha} N^{(n2)}_{j,\beta} W^k_{m1\,n2} J^{k\tau s} + C^k_{66} N^{(m3)}_{i,\beta} N^{(n3)}_{j,\alpha} W^k_{m3\,n3} J^{k\tau s} +$$
$$+ C^k_{16} N^{(m1)}_{i,\alpha} N^{(n3)}_{j,\alpha} W^k_{m1\,n3} J^{k\tau s}_{\frac{\beta}{\alpha}} + \frac{C^k_{45}}{R^k_\alpha R^k_\beta} N^{(m1)}_i N^{(n2)}_j W^k_{m1\,n2} J^{k\tau s}$$
$$(37)$$

$$K^{k\tau sij}_{\alpha z} = C^k_{45} N^{(m1)}_i N^{(n2)}_{j,\beta} W^k_{m1\,n2} J^{k\tau_z s}_\alpha + C^k_{55} N^{(m1)}_i N^{(n1)}_{j,\alpha} W^k_{m1\,n1} J^{k\tau_z s}_\beta + C^k_{36} N^{(m3)}_{i,\beta} W^k_{m3\,j} J^{k\tau s_z}_\alpha +$$
$$+ C^k_{13} N^{(m1)}_{i,\alpha} W^k_{m1\,j} J^{k\tau s_z}_\beta - \frac{C^k_{45}}{R^k_\alpha} N^{(m1)}_i N^{(n2)}_{j,\beta} W^k_{m1\,n2} J^{k\tau s} - \frac{C^k_{55}}{R^k_\alpha} N^{(m1)}_i N^{(n1)}_{j,\alpha} W^k_{m1\,n1} J^{k\tau s}_{\frac{\beta}{\alpha}} +$$
$$+ \frac{C^k_{26}}{R^k_\beta} N^{(m3)}_{i,\beta} N^{(n2)}_j W^k_{m3\,n2} J^{k\tau s}_{\frac{\alpha}{\beta}} + \frac{C^k_{16}}{R^k_\alpha} N^{(m3)}_{i,\beta} N^{(n1)}_j W^k_{m3\,n1} J^{k\tau s} + \frac{C^k_{12}}{R^k_\beta} N^{(m1)}_{i,\alpha} N^{(n2)}_j W^k_{m1\,n2} J^{k\tau s} +$$
$$+ \frac{C^k_{11}}{R^k_\alpha} N^{(m1)}_{i,\alpha} N^{(n1)}_j W^k_{m1\,n1} J^{k\tau s}_{\frac{\beta}{\alpha}}$$
$$(38)$$

$$K^{k\tau sij}_{\beta\alpha} = C^k_{45} N^{(m2)}_i N^{(n1)}_j W^k_{m2\,n1} J^{k\tau_z s_z}_{\alpha\beta} - \frac{C^k_{45}}{R^k_\alpha} N^{(m2)}_i N^{(n1)}_j W^k_{m2\,n1} J^{k\tau_z s}_\beta - \frac{C^k_{45}}{R^k_\beta} N^{(m2)}_i N^{(n1)}_j W^k_{m2\,n1} J^{k\tau s_z}_\alpha +$$
$$+ C^k_{26} N^{(m2)}_{i,\beta} N^{(n3)}_{j,\beta} W^k_{m2\,n3} J^{k\tau s}_{\frac{\alpha}{\beta}} + C^k_{66} N^{(m3)}_{i,\alpha} N^{(n3)}_{j,\beta} W^k_{m3\,n3} J^{k\tau s} + C^k_{12} N^{(m2)}_{i,\beta} N^{(n1)}_{j,\alpha} W^k_{m2\,n1} J^{k\tau s} +$$
$$+ C^k_{16} N^{(m3)}_{i,\alpha} N^{(n1)}_{j,\alpha} W^k_{m3\,n1} J^{k\tau s}_{\frac{\beta}{\alpha}} + \frac{C^k_{45}}{R^k_\alpha R^k_\beta} N^{(m2)}_i N^{(n1)}_j W^k_{m2\,n1} J^{k\tau s}$$
$$(39)$$

$$K_{\beta\beta}^{k\tau sij} = C_{44}^k \, N_i^{(m2)} N_j^{(n2)} \, W_{m2\,n2}^k \, J_{\alpha\beta}^{k\tau_z s_z} - \frac{C_{44}^k}{R_\beta^k} \, N_i^{(m2)} N_j^{(n2)} \, W_{m2\,n2}^k \, J_\alpha^{k\tau_z s} - \frac{C_{44}^k}{R_\beta^k} \, N_i^{(m2)} N_j^{(n2)} \, W_{m2\,n2}^k \, J_\alpha^{k\tau s_z} +$$

$$+ \, C_{22}^k \, N_{i,\beta}^{(m2)} N_{j,\beta}^{(n2)} \, W_{m2\,n2}^k \, J_{\frac{\alpha}{\beta}}^{k\tau s} + C_{26}^k \, N_{i,\alpha}^{(m3)} N_{j,\beta}^{(n2)} \, W_{m3\,n2}^k \, J^{k\tau s} + C_{26}^k \, N_{i,\beta}^{(m2)} N_{j,\alpha}^{(n3)} \, W_{m2\,n3}^k \, J^{k\tau s} +$$

$$+ \, C_{66}^k \, N_{i,\alpha}^{(m3)} N_{j,\alpha}^{(n3)} \, W_{m3\,n3}^k \, J_{\frac{\beta}{\alpha}}^{k\tau s} + \frac{C_{44}^k}{\left(R_\beta^k\right)^2} \, N_i^{(m2)} N_j^{(n2)} \, W_{m2\,n2}^k \, J_{\frac{\alpha}{\beta}}^{k\tau s}$$

$$(40)$$

$$K_{\beta z}^{k\tau sij} = C_{44}^k \, N_i^{(m2)} N_{j,\beta}^{(n2)} \, W_{m2\,n2}^k \, J_\alpha^{k\tau_z s} + C_{45}^k \, N_i^{(m2)} N_{j,\alpha}^{(n1)} \, W_{m2\,n1}^k \, J_\beta^{k\tau_z s} + C_{23}^k \, N_{i,\beta}^{(m2)} \, W_{m2\,j}^k \, J_\alpha^{k\tau s_z} +$$

$$+ \, C_{36}^k \, N_{i,\alpha}^{(m3)} \, W_{m3\,j}^k \, J_\beta^{k\tau s_z} - \frac{C_{44}^k}{R_\beta^k} \, N_i^{(m2)} N_{j,\beta}^{(n2)} \, W_{m2\,n2}^k \, J_{\frac{\alpha}{\beta}}^{k\tau s} - \frac{C_{45}^k}{R_\beta^k} \, N_i^{(m2)} N_{j,\alpha}^{(n1)} \, W_{m2\,n1}^k \, J^{k\tau s} +$$

$$+ \, \frac{C_{22}^k}{R_\beta^k} \, N_{i,\beta}^{(m2)} N_j^{(n2)} \, W_{m2\,n2}^k \, J_{\frac{\alpha}{\beta}}^{k\tau s} + \frac{C_{12}^k}{R_\alpha^k} \, N_{i,\beta}^{(m2)} N_j^{(n1)} \, W_{m2\,n1}^k \, J^{k\tau s} + \frac{C_{26}^k}{R_\beta^k} \, N_{i,\alpha}^{(m3)} N_j^{(n2)} \, W_{m3\,n2}^k \, J^{k\tau s} +$$

$$+ \, \frac{C_{16}^k}{R_\alpha^k} \, N_{i,\alpha}^{(m3)} N_j^{(n1)} \, W_{m3\,n1}^k \, J_{\frac{\beta}{\alpha}}^{k\tau s}$$

$$(41)$$

$$K_{z\alpha}^{k\tau sij} = C_{36}^k \, N_{j,\beta}^{(n3)} \, W_{i\,n3}^k \, J_\alpha^{k\tau_z s} + C_{13}^k \, N_{j,\alpha}^{(n1)} \, W_{i\,n1}^k \, J_\beta^{k\tau_z s} + C_{45}^k \, N_{i,\beta}^{(m2)} N_j^{(n1)} \, W_{m2\,n1}^k \, J_\alpha^{k\tau s_z} +$$

$$+ \, C_{55}^k \, N_{i,\alpha}^{(m1)} N_j^{(n1)} \, W_{m1\,n1}^k \, J_\beta^{k\tau s_z} + \frac{C_{26}^k}{R_\beta^k} \, N_i^{(m2)} N_{j,\beta}^{(n3)} \, W_{m2\,n3}^k \, J_{\frac{\alpha}{\beta}}^{k\tau s} + \frac{C_{16}^k}{R_\alpha^k} \, N_i^{(m1)} N_{j,\beta}^{(n3)} \, W_{m1\,n3}^k \, J^{k\tau s} +$$

$$+ \, \frac{C_{12}^k}{R_\beta^k} \, N_i^{(m2)} N_{j,\alpha}^{(n1)} \, W_{m2\,n1}^k \, J^{k\tau s} + \frac{C_{11}^k}{R_\alpha^k} \, N_i^{(m1)} N_{j,\alpha}^{(n1)} \, W_{m1\,n1}^k \, J_{\frac{\beta}{\alpha}}^{k\tau s} - \frac{C_{45}^k}{R_\alpha^k} \, N_{i,\beta}^{(m2)} N_j^{(n1)} \, W_{m2\,n1}^k \, J^{k\tau s} -$$

$$- \, \frac{C_{55}^k}{R_\alpha^k} \, N_{i,\alpha}^{(m1)} N_j^{(n1)} \, W_{m1\,n1}^k \, J_{\frac{\beta}{\alpha}}^{k\tau s}$$

$$(42)$$

$$K_{z\beta}^{k\tau sij} = C_{23}^k \, N_{j,\beta}^{(n2)} \, W_{i\,n2}^k \, J_\alpha^{k\tau_z s} + C_{36}^k \, N_{j,\alpha}^{(n3)} \, W_{i\,n3}^k \, J_\beta^{k\tau_z s} + C_{44}^k \, N_{i,\beta}^{(m2)} N_j^{(n2)} \, W_{m2\,n2}^k \, J_\alpha^{k\tau s_z} +$$

$$+ \, C_{45}^k \, N_{i,\alpha}^{(m1)} N_j^{(n2)} \, W_{m1\,n2}^k \, J_\beta^{k\tau s_z} + \frac{C_{22}^k}{R_\beta^k} \, N_i^{(m2)} N_{j,\beta}^{(n2)} \, W_{m2\,n2}^k \, J_{\frac{\alpha}{\beta}}^{k\tau s} + \frac{C_{12}^k}{R_\alpha^k} \, N_i^{(m1)} N_{j,\beta}^{(n2)} \, W_{m1\,n2}^k \, J^{k\tau s} +$$

$$+ \, \frac{C_{26}^k}{R_\beta^k} \, N_i^{(m2)} N_{j,\alpha}^{(n3)} \, W_{m2\,n3}^k \, J^{k\tau s} + \frac{C_{16}^k}{R_\alpha^k} \, N_i^{(m1)} N_{j,\alpha}^{(n3)} \, W_{m1\,n3}^k \, J_{\frac{\beta}{\alpha}}^{k\tau s} - \frac{C_{44}^k}{R_\beta^k} \, N_{i,\beta}^{(m2)} N_j^{(n2)} \, W_{m2\,n2}^k \, J_{\frac{\alpha}{\beta}}^{k\tau s} -$$

$$- \, \frac{C_{45}^k}{R_\beta^k} \, N_{i,\alpha}^{(m1)} N_j^{(n2)} \, W_{m1\,n2}^k \, J^{k\tau s}$$

$$(43)$$

$$
\begin{aligned}
K_{zz}^{k\tau sij} = {} & C_{33}^k \, W_{ij}^k \, J_{\alpha\beta}^{k\tau_z s_z} + \frac{C_{23}^k}{R_\beta^k} \, N_j^{(n2)} \, W_{i\,n2}^k \, J_\alpha^{k\tau_z s} + \frac{C_{13}^k}{R_\alpha^k} \, N_j^{(n1)} \, W_{i\,n1}^k \, J_\beta^{k\tau_z s} + \\[2mm]
& + \frac{C_{23}^k}{R_\beta^k} \, N_i^{(m2)} \, W_{m2\,j}^k \, J_\alpha^{k\tau s_z} + \frac{C_{13}^k}{R_\alpha^k} \, N_i^{(m1)} \, W_{m1\,j}^k \, J_\beta^{k\tau s_z} + C_{44}^k \, N_{i,\beta}^{(m2)} N_{j,\beta}^{(n2)} \, W_{m2\,n2}^k \, J_{\frac{\alpha}{\beta}}^{k\tau s} + \\[2mm]
& + C_{45}^k \, N_{i,\alpha}^{(m1)} N_{j,\beta}^{(n2)} \, W_{m1\,n2}^k \, J^{k\tau s} + C_{45}^k \, N_{i,\beta}^{(m2)} N_{j,\alpha}^{(n1)} \, W_{m2\,n1}^k \, J^{k\tau s} + C_{55}^k \, N_{i,\alpha}^{(m1)} N_{j,\alpha}^{(n1)} \, W_{m1\,n1}^k \, J_{\frac{\beta}{\alpha}}^{k\tau s} + \\[2mm]
& + \frac{C_{12}^k}{R_\alpha^k \, R_\beta^k} \, N_i^{(m1)} N_j^{(n2)} \, W_{m1\,n2}^k \, J^{k\tau s} + \frac{C_{12}^k}{R_\alpha^k \, R_\beta^k} \, N_i^{(m2)} N_j^{(n1)} \, W_{m2\,n1}^k \, J^{k\tau s} + \\[2mm]
& + \frac{C_{22}^k}{\left(R_\beta^k\right)^2} \, N_i^{(m2)} N_j^{(n2)} \, W_{m2\,n2}^k \, J_{\frac{\alpha}{\beta}}^{k\tau s} + \frac{C_{11}^k}{\left(R_\alpha^k\right)^2} \, N_i^{(m1)} N_j^{(n1)} \, W_{m1\,n1}^k \, J_{\frac{\beta}{\alpha}}^{k\tau s}
\end{aligned} \tag{44}
$$

Tables

Table 1: Cylindrical shell. Convergence study in terms of $\omega \times 10\sqrt{\rho h^2/E_T}$ for different circumferential wave numbers n. Comparison to three-dimensional solutions by Noor and Rarig [60]. $E_L/E_T = 30$, $a/R_\beta = 1$, $h/R_\beta = 0.05$, $m = 1$ and $N_l = 2$. Lamination $(90^o/0^o)$.

Mesh	4×4	8×8	4×8	4×12	4×16	4×20	4×22	$3D$
$n = 2$	0.8114	0.8162	0.8163	0.8167	0.8167	0.8167	0.8167	0.8165
$n = 4$	-	0.5877	0.5877	0.5378	0.5384	0.5386	0.5386	0.5385
$n = 6$	-	0.4280	0.4281	0.4194	0.4211	0.4216	0.4217	0.4218

Table 2: Cylindrical shell two layered. Effect of degree of orthotropy of the individual layers E_L/E_T on $\omega \times 10\sqrt{\rho h^2/E_T}$. Comparison to three-dimensional solutions by Noor and Rarig [60]. $h/R_\beta = 0.2$, $a/R_\beta = 1$ and $m = 1$, $n = 4$. Lamination $(90^o/0^o)$.

3D [60]	2.3141	2.5464	2.9262
E_L/E_T	3	10	40
L4	2.3148	2.5472	2.9274
L1	2.3300	2.5634	2.9676
EZ3	2.3155	2.5512	2.9579
E4	2.3155	2.5495	2.9424
E2	2.3231	2.5601	2.9833
FSDT	2.3305	2.5733	3.0617
CLT	2.3867	2.6539	3.1033

Table 3: Cylindrical shell. Effect of the thickness to radii ratio h/R_β on $\omega \times 10\sqrt{\rho h^2/E_T}$. Comparison to three-dimensional solutions by Noor and Rarig [60]. $E_L/E_T = 30$, $a/R_\beta = 1$, $m = 1$ and $N_l = 2$. Lamination $(90^o/0^o)$.

	$h/R_\beta = 0.05$			$h/R_\beta = 0.25$			$h/R_\beta = 0.40$		
3D [60]	0.8165	0.5385	0.4218	4.4910	3.8047	4.1584	7.5953	6.9568	7.9209
n	2	4	6	2	4	6	2	4	6
L4	0.8167	0.5386	0.4217	4.4933	3.8064	4.1603	7.6007	6.9609	7.9255
L1	0.8169	0.5390	0.4224	4.5262	3.8643	4.2448	7.6963	7.1168	8.1350
EZ3	0.8168	0.5387	0.4219	4.5195	3.8465	4.2108	7.6703	7.0634	8.0458
E4	0.8168	0.5387	0.4218	4.5062	3.8263	4.1849	7.6355	7.0103	7.9847
E2	0.8169	0.5389	0.4221	4.5409	3.8825	4.2663	7.7443	7.1772	8.2034
FSDT	0.8175	0.5393	0.4227	4.6090	3.8828	4.4149	7.9973	7.5512	8.6757
CLT	0.8177	0.5398	0.4241	5.1142	3.8838	4.8132	9.3605	9.0851	9.3924

Table 4: Spherical square cross-ply panels, simply supported. Effect of radii to length ratio R/a on $\omega\sqrt{\rho a^4/h^2 E_T}$. Comparison to various theories. $E_L/E_T = 25$, $G_{LT}/E_T = 0.5$, $G_{TT}/E_T = 0.2$, $\nu_{LT} = \nu_{TT} = 0.25$, $a/h = 10$ and $m = 1$, $n = 1$. Mesh 16×16. Lamination $(0^o/90^o/0^o)$.

R/a	1	2	5	10	plate
$L4_a$	15.680	12.773	11.685	11.515	11.457
HSDT [62]	–	–	12.060	11.860	11.790
FSDT [63]	16.115	13.382	12.372	12.215	12.162
CLT [64]	17.820	15.878	15.233	15.136	15.104
L4	15.680	12.773	11.685	11.515	11.457
L1	15.750	12.877	11.804	11.636	11.580
EZ3	15.690	12.780	11.689	11.518	11.460
E4	15.830	13.018	11.973	11.811	11.756
E2	16.235	13.656	12.717	12.572	12.523
FSDT	16.299	13.684	12.725	12.577	12.527
CLT	17.745	15.879	15.234	15.137	15.104

Table 5: Spherical square cross-ply panels. Boundary conditions: Clamped/Free/Clamped/Free. Effect of radii to length ratio R/a and radii to thickness ratio R/h on $\omega\sqrt{\rho a^4/h^2\,E_T}$. $E_L/E_T = 25$, $G_{LT}/E_T = 0.5$, $G_{TT}/E_T = 0.2$, $\nu_{LT} = \nu_{TT} = 0.25$, $m = 1$, $n = 1$. Mesh 16×16. Lamination $(0^o/90^o/0^o)$.

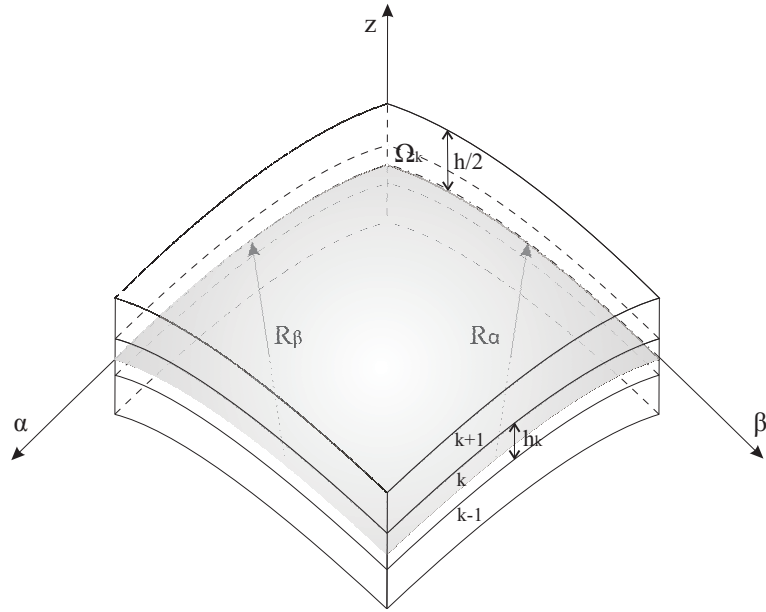|	$R/a = 1$			$R/a = 10$		
R/h	2.5	4	20	25	40	200
L4	5.126	8.454	42.895	4.667	7.094	23.505
L1	5.172	8.498	42.930	4.786	7.263	23.769
EZ3	5.168	8.497	42.919	4.755	7.188	23.524
E4	5.159	8.483	42.933	4.761	7.249	24.139
E2	5.175	8.504	43.012	4.992	7.852	25.868
FSDT	5.189	8.520	43.020	4.994	7.854	25.867
CLT	5.255	8.570	43.202	5.429	8.688	32.440

Figures

Figure 1: Multilayered doubly-curved shell: notation and geometry.
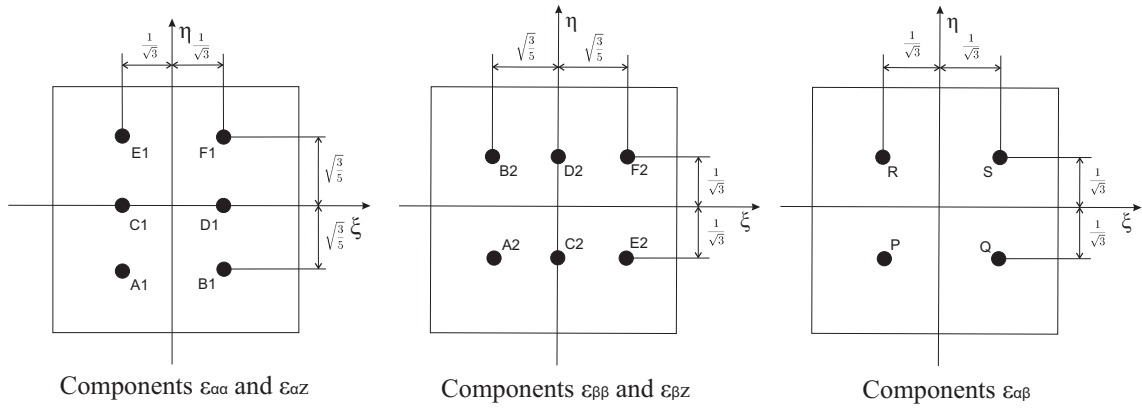
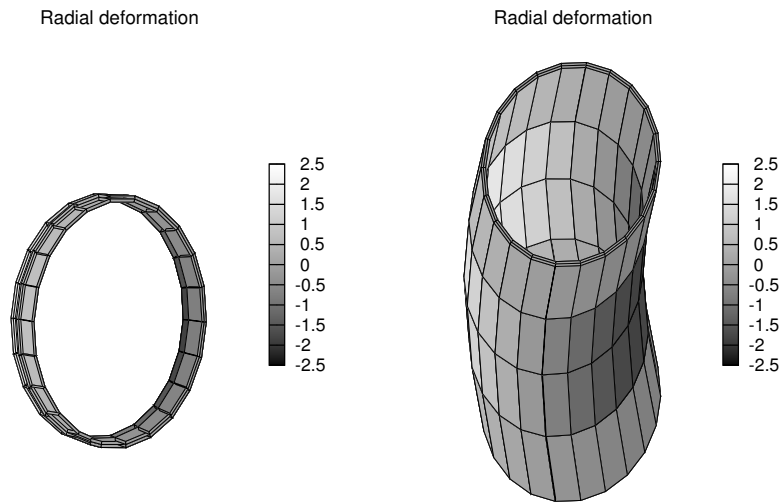Figure 2: Tying points for the MITC9 shell element.

Figure 3: Two-layered cylinder, 2 circumferential half-waves.
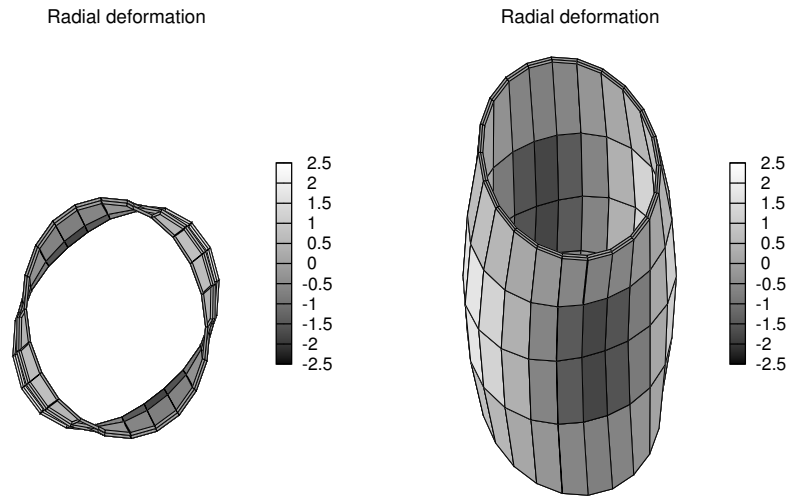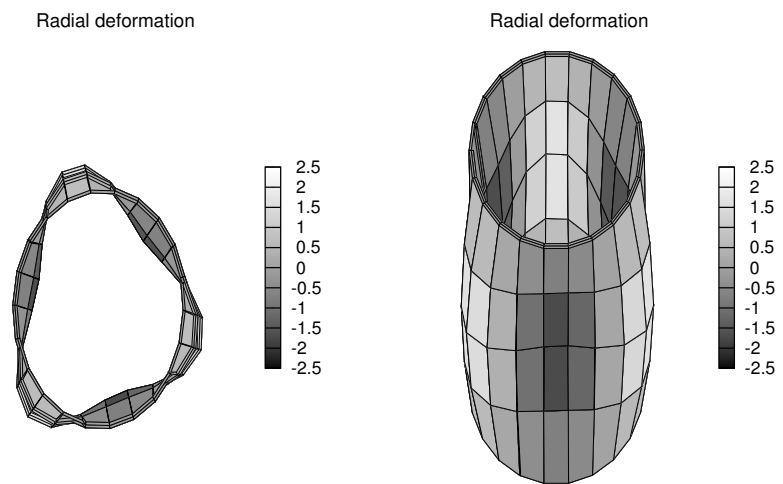
Figure 4: Two-layered cylinder, 4 circumferential half-waves.

Figure 5: Two-layered cylinder, 6 circumferential half-waves.